Int. J. Exp. Path. (2009), 90, 587–597
doi: 10.1111/j.1365-2613.2009.00679.x

ORIGINAL ARTICLE

Gamma–delta T cell subsets are differentially associated with granuloma development and organization in a bovine model of mycobacterial disease

Brandon L. Plattner*, Robert T. Doyle† and Jesse M. Hostetter*

*Department of Veterinary Pathology, College of Veterinary Medicine, Iowa State University, Ames, IA, USA and †Department of Genetics, Development and Cell Biology, RJ Carver Laboratory for Ultrahigh Resolution Biological Microscopy, Iowa State University, Ames, IA, USA

INTERNATIONAL JOURNAL OF EXPERIMENTAL PATHOLOGY

Received for publication:
27 February 2009
Accepted for publication:
5 June 2009

Correspondence:
Jesse M. Hostetter
2720 Veterinary Medicine
Department of Veterinary Pathology
College of Veterinary Medicine
Iowa State University
Ames
IA 50011-1250
USA
Tel.: +1 515 2943282
Fax: +1 515 2945423
E-mail: jesseh@iastate.edu

Summary

The characteristic lesion in bovine tuberculosis is well-organized respiratory granulomas. This is typically associated with a strong T-helper 1 biased cell-mediated immune response and eventual containment of the infection. In bovine paratuberculosis, the classic lesion is unorganized granulomatous intestinal inflammation. Clinical paratuberculosis is associated with a T-helper 2 biased humoral immune response and eventual death because of inability of the host to contain the infection. Recent reports have suggested that gamma–delta (γδ) T cells play a significant role in granuloma development and/or maintenance during initial stages of infection and may influence the subsequent adaptive immune response. The objective of this study was to use an *in vivo* bovine model to evaluate γδ T cells during the early host immune response to mycobacterial infection. We used immunofluorescent staining, hyperspectral microscopy, and computerized assisted morphometry to evaluate staining and distribution of γδ T cells during development of organized and unorganized granulomas. Our data suggest that bovine γδ T cell subsets are differentially recruited to early infection sites, and may be instrumental during the initial anti-mycobacterial host immune response as well as for granuloma organization.

Keywords
bovine, gamma–delta T cells, granuloma, mycobacteria, paratuberculosis

The role of major T lymphocyte subsets is well documented in both tuberculous and non-tuberculous mycobacterial disease (Co *et al.* 2004; Saunders & Britton 2007); however, recent studies in humans (Battistini *et al.* 2005; Puan *et al.* 2007), non-human primates (Shen *et al.* 2002) and cattle (Wangoo *et al.* 2005; Price *et al.* 2007; Johnson *et al.* 2008; Price & Hope 2008) have provided evidence that minor T cell populations including gamma–delta (γδ) T cells are also involved. It is thought that γδ T cells play an early role during infection and provide a link between the innate and adaptive immune responses (Liebana *et al.* 2000; Brandes *et al.* 2005). It is known that γδ T cells differ widely between species, and interspecies correlation of the data has not been reported; however, human and bovine γδ T cells

share some notable features including subset-specific tissue distribution (Machugh *et al.* 1997; Das *et al.* 2004) and proposed function (Morita *et al.* 1995; Hedges *et al.* 2005). Human γδ T cell subsets are distinguished by germ-line gene segment usage and are thought to represent a heterogenous population of cells capable of serving immediate effector, tissue homing, recall or even memory functions (Dieli *et al.* 2003; Battistini *et al.* 2005). Bovine γδ T cell subsets are differentiated by a unique workshop cluster 1 (WC1) molecule which is a member of the scavenger receptor cysteine rich family and is expressed on the surface of 50–90% of peripheral blood γδ T cells (Blumerman *et al.* 2006). Distinct isoforms of the WC1 molecule have been characterized (Wijngaard *et al.* 1994; Rogers *et al.* 2005a,b), yet its exact function remains unknown. Work by Jutila and colleagues has suggested that bovine WC1 + γδ T cells have inflammatory characteristics while WC1- cells have a regulatory function (Hedges *et al.* 2003; Meissner *et al.* 2003). A role for γδ T cells during antimycobacterial immunity is implied as WC1 + γδ T cells from either infected or uninfected cattle proliferate and produce interferon-γ when stimulated with *M. bovis* antigens (Smyth *et al.* 2001; Welsh *et al.* 2002). The importance of WC1 + γδ T cells is further supported by studies showing modulation of the immune response in calves depleted of WC1 + γδ T cells (Kennedy *et al.* 2002). Evidence that γδ T cells play a significant role at initial infection sites is less clear, but these cells are observed within mycobacteria-induced lesions of humans and cattle (Modlin *et al.* 1989; Wilson *et al.* 1999; Dieli *et al.* 2003) and in lymph nodes draining mycobacterial infection sites of cattle (Wangoo *et al.* 2005; Liebana *et al.* 2007; Palmer *et al.* 2007). A role for γδ T cells during granuloma development in mice or as early effectors during mycobacterial infection of humans and macaques is supported by recent reports (Hoft *et al.* 1998; Tanaka *et al.* 2000; Shen *et al.* 2002; Chen & Letvin 2003).

It is generally accepted that progression of mycobacterial disease is influenced at the level of the infection site and that survival of the host depends on the ability to limit mycobacterial proliferation through effective granuloma formation (Russell 2007). Well-organized lesions correlate with longer host survival while unorganized lesions are associated with a poorer prognosis, and this suggests that the local host tissue response is indicative of a patient's likely response to therapy and long-term survival (Emile *et al.* 1997; Lammas *et al.* 2002; Saunders & Britton 2007). A variety of *in vivo* and *in vitro* animal model systems have been utilized to further characterize the complex immunopathology of the infection site with variable success. The murine model has limitations for understanding granuloma development and progression in response to mycobacterial infection (Russell 2007). The bovine is an attractive alternative model system (Endsley *et al.* 2009), and cattle are natural hosts of tuberculous and non-tuberculous mycobacterial infections.

The goal of the current study was to evaluate γδ T cell subsets in mycobacterial granulomas to better understand the early role of these cells in host defence against infection. A bovine subcutaneous model was employed to address two fundamental questions concerning the relationship of γδ T cells to the developing granuloma during mycobacterial infection. First, we sought to identify differences in γδ T cell recruitment into initial stages of organized *vs.* unorganized granulomas. Second, we asked if the ability of an animal to initially generate an organized granuloma to *Mycobacterium avium* subspecies *paratuberculosis (Map)* antigens (killed bacterin vaccine) would translate into the development of an organized granuloma at a subsequent focus of *Map* infection. Our data support the initial hypothesis that γδ T cell subsets are differentially associated with organized and unorganized granulomatous lesions in the bovine. Data from these experiments suggest that bovine γδ T cell subsets have different immune roles, and may be central regulators of both local and systemic antimycobacterial immune responses.

Materials and methods

Animals and care

Four- to 6-week-old castrated male Holstein calves were used in the following experiments and were housed in isolation at the Iowa State University College of Veterinary Medicine biosafety level II animal care facility. A total of nine calves were used for this project and were maintained three at a time for handling purposes. Animals were acquired from the Iowa State University dairy research farm (Ankeny, IA, USA), a herd certified free of *Map* infection. All live animal-related protocols were approved by the Committee on Animal Care and Use at Iowa State University.

Vaccine

M. avium subspecies *paratuberculosis* bacterin (Mycopar®; Fort Dodge Animal Health Company, Fort Dodge, IA, USA) was used in this experiment. Mycopar® is a commercially available whole-cell bacterin containing inactivated *Mycobacterium paratuberculosis* in oil. Mycopar® is known to generate a variably sized granuloma *in vivo*, and as such was used in these experiments as an example of a highly organized (tuberculoid-like) granuloma allowable in biosafety level II facilities.

Bacterial inoculum and infection

The *Map* strain 19698 was obtained from the American Type Culture Collection (Manassas, VA, USA) and maintained in Middlebrook 7H9 broth supplemented with mycobactin J. Logarithmic growth-phase bacteria were washed and resuspended in sterile saline for inoculation. Bacterial concentration was determined by measuring absorbance at 540 nm, comparing the absorbance optical density to the standard curve and adjusted to a final concentration of 1×10^9 CFU/ml in 0.9% sterile saline solution. The *Map* inoculum used in these studies was shown to have greater than 90% viability via fluorescein diacetate staining and flow cytometry analysis prior to inoculation. In addition, challenge inocula were confirmed negative for contaminants by streaking onto sheep blood agar plates 24 h prior to injection.

Monoclonal antibodies and antigens

The following mouse anti-bovine monoclonal antibodies were purchased from VMRD (Pullman, WA, USA) and used to characterize γδ T cells by multicolour fluorescent immunohistochemistry: anti-γδ T cell receptor (TCR) (GB21A), anti-WC1(n1) (B7A1). Alexa-fluor 555-conjugated goat anti-mouse IgG2b and Alexa-fluor 488-conjugated goat anti-mouse IgM (Invitrogen Molecular Probes, Carlsbad, CA, USA) were used as secondary antibody conjugates. 4′,6-diamidino-2-phenylindole (DAPI) nucleic acid stain (Invitrogen Molecular Probes) was used to stain nuclei.

Experimental design

For these experiments, a localized *Map* infection system developed in our laboratory was used with a few modifications (Simutis *et al*. 2005; Lei *et al*. 2008). Calves were inoculated on day 0 of the experiment with either *Map* vaccine ($n = 6$) or sterile saline ($n = 3$) in the following manner: 250 μl was administered subcutaneously in three locations separated by 8–10 cm in the left cervical region. A single vaccine injection site nodule was surgically removed from each calf at three postinoculation time points designated early (7–10 days), middle (30 days) and late (greater than 60 days).

Calves were then inoculated with live *Map* 60 days following Mycopar® or sham saline vaccination. Each calf was subcutaneously inoculated with 5×10^8 live *Map* in 500 μl sterile saline in three locations separated by 8–10 cm in the right cervical region. A *Map* infection site nodule was surgically removed from each calf at three postinoculation time points designated early (7–10 days), middle (30 days) and late (greater than 60 days). All tissues were fixed for histopathology in 10% neutral-buffered formalin or snap-frozen for immunofluorescence in liquid Tissue-Tek Cryo-OCT compound (Fisher Scientific, Pittsburgh, PA, USA) and stored at −80 °C.

Scoring of haematoxylin and eosin stained lesions

Formalin-fixed, paraffin-embedded vaccine and infection site lesions were sectioned (4 μm) and stained with haematoxylin and eosin for histologic evaluation and lesion scoring. Haematoxylin and eosin stained vaccine and infection site lesions were individually scored using a scoring system adapted from previous studies (Wangoo *et al*. 2005; Johnson *et al*. 2006; Lei *et al*. 2008). Scores of 0–3 were assigned for each parameter to reflect the degree and organization within each lesion. A score of 0 indicates absence of the parameter from the lesion (normal), while a score of 3 reflects both a significant presence (most severe) and a high degree of organization of the parameter within the lesion. The following parameters were evaluated: fibrous connective tissue, macrophages, polymorphonuclear cells (neutrophils and eosinophils), small mononuclear cells (lymphocytes and plasma cells), multinucleated giant cells, necrosis and mineralization. Individual parameter scores were summated, and a single collective score was assigned for each lesion which reflected the histological organization and stage of development of each lesion. Negative control sites (saline) lacked significant inflammatory components.

Immunofluorescent tissue staining

Frozen sections (OCT) were cut at 4 μm and fixed in 100% ice-cold ethanol. Sections were washed once with phosphate-buffered saline (0.01 M PBS, pH 7.2), blocked for 30 min with 10% normal goat serum, then stained at 4 °C overnight with a cocktail containing monoclonal antibodies for γδ TCR (1/10,000) and WC1 (1/1000). Slides were then washed twice with sterile PBS and stained for 45 min at 20 °C sequentially with appropriate secondary conjugates (AF555 goat anti-mouse IgG2b and AF488 goat anti-mouse IgM, 1/1000), prior to nuclei staining with DAPI (1/30,000). Following staining, slides were washed twice with sterile PBS, then mounted with anti-fade medium [4% *n*-propyl gallate (Sigma Aldrich, St Louis, MO, USA) in 90% glycerol and 10% PBS] and cover-slipped.

Immunofluorescent hyperspectral microscopy

Fluorescence image data was collected using an Optical Insights hyperspectral microscopy system composed of the Optical Insights (MAG Biosystems, Tucson, AZ, USA)

instrument attached to an inverted Nikon TE2000 microscope (Nikon, Melville, NY, USA) equipped with a Photometrics Cascade 512B digital camera and Melange® software (Molecular Devices, Sunnyvale, CA, USA). All images were captured at 200 × magnification (20 × objective). Fluorescence data were first collected from single-colour (AF488, AF555 or DAPI) stained slides, and individual fluorescent spectra were defined. Sample slides stained with all three fluorophores were then imaged. Raw data were corrected for tissue autofluorescence, and hyperspectral unmixing was performed to extract individual spectra based on the previously defined parameters for each fluorescent spectra.

Computer-assisted morphometric analysis of immunofluorescent stained slides

Image analysis was performed using Metamorph 7.0 software (Molecular Devices). Briefly, multicolour images were separated based on their unmixed and corrected spectral profiles. A visual threshold was applied to individual spectral profiles, and object definition was defined in pixels based on the scorer's (BLP) visual interpretation of a single positive cell. Data from individual images were then collected and stored as the following parameters: total cell count (DAPI positive nuclei per image), total γδ TCR positive cells (AF555-expressing cells) and total WC1 positive cells (AF488-expressing cells per image).

Statistical analysis

Statistical analysis was performed using JMP 7.0.2 Statistical Discovery system (SAS Institute, Cary, NC, USA). Data are presented as the mean value ± standard error of the mean except where stated otherwise. Student's *t*-test and one-way ANOVA were used for the statistical analysis. Group mean differences were considered significant if the *P*-value was <0.05.

Results

Differential histopathology of subcutaneous granulomas

To generate unorganized and organized granulomas, we inoculated either live *Map* organisms or *Map* vaccine subcutaneously in calves. *Map* inoculation site nodules reached a maximal size of 20–25 mm diameter approximately 7–10 days postinjection and gradually resolved. *Map* vaccine site nodules reached a maximal size of 30–50 mm diameter approximately 20–30 days postinjection and generally remained grossly unchanged in size for the study duration

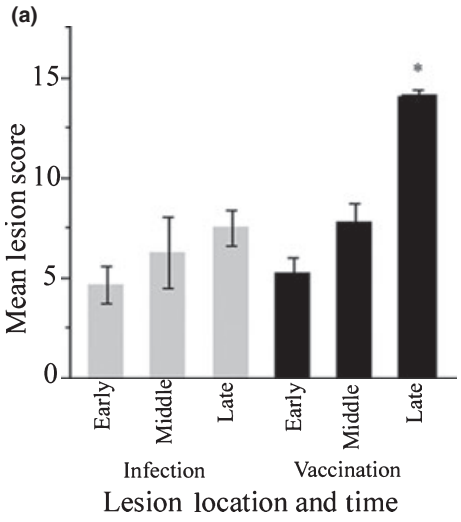

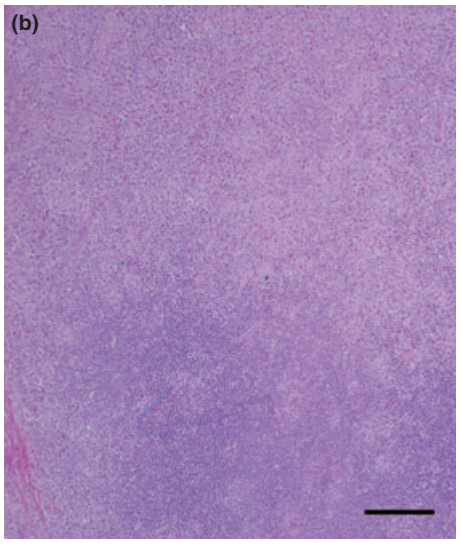

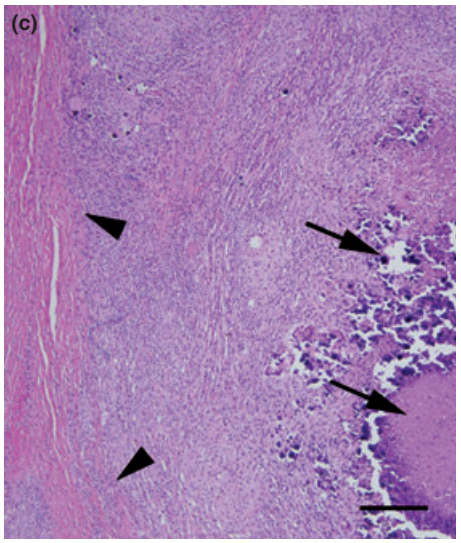

Figure 1 Histology of unorganized and highly organized granulomas. Panel (a) summarizes lesion scores for infection sites (grey bars) and vaccination sites (black bars). Late stage vaccine sites scored significantly higher than all other sites (*P < 0.0023). Late stage live *Map* infection sites (b) were unorganized sheets of macrophages and lymphocytes without central necrosis or peripheral fibrosis. Late stage vaccine sites (c) were highly organized with macrophages and lymphocytes oriented around central lakes of necrotic debris (arrows) with mineral. Granulomas were encircled by a prominent fibrous capsule (arrowheads). Bar = 200 μm.

(data not shown). Histopathology observed at *Map* inoculation sites was similar to intestinal lesions of cattle with naturally occurring cases of *Map* infection (Johne's disease) and was characterized by an unorganized accumulation of macrophages with fewer lymphocytes and plasma cells. The lesions did not exhibit significant histologic progression over time (Figure 1a), and at later stages diffuse granulomatous lesions lacked fibrous tissue encapsulation, central necrosis and mineralization (Figure 1b). Initial lesions at *Map* vaccine sites were similar to infection sites; however, in contrast to *Map* infection sites, they became highly organized over time (Figure 1a; *P < 0.0023). Features of later stage granulomas included central coagulative to lytic cellular necrosis with variable degrees of mineralization surrounded by a dense rim of macrophages, giant cells and aggregates of lymphocytes and plasma cells. The entire nodular structure was eventually rimmed by a band of mature dense fibrous tissue (Figure 1c).

γδ T cell subsets in unorganized and highly organized granulomas

We compared γδ T cell subsets during developing stages of highly organized and unorganized granulomatous lesions using immunofluorescence staining and computer-assisted morphometry. In unorganized lesions, the total number of recruited γδ T cells was significantly greater in late stages compared to early stages (Figure 2a; *P = 0.0002). Compared to unorganized lesions, highly organized granulomas contained significantly higher numbers of WC1 + cells during initial stages (Figure 2b; *P = 0.0062) and WC1- cells during later stages (Figure 2c; **P = 0.0017).

Spatial organization of γδ T cell subsets in granulomas

We evaluated spatial orientation and arrangement of γδ T cell subsets within developing granuloma subtypes. Early

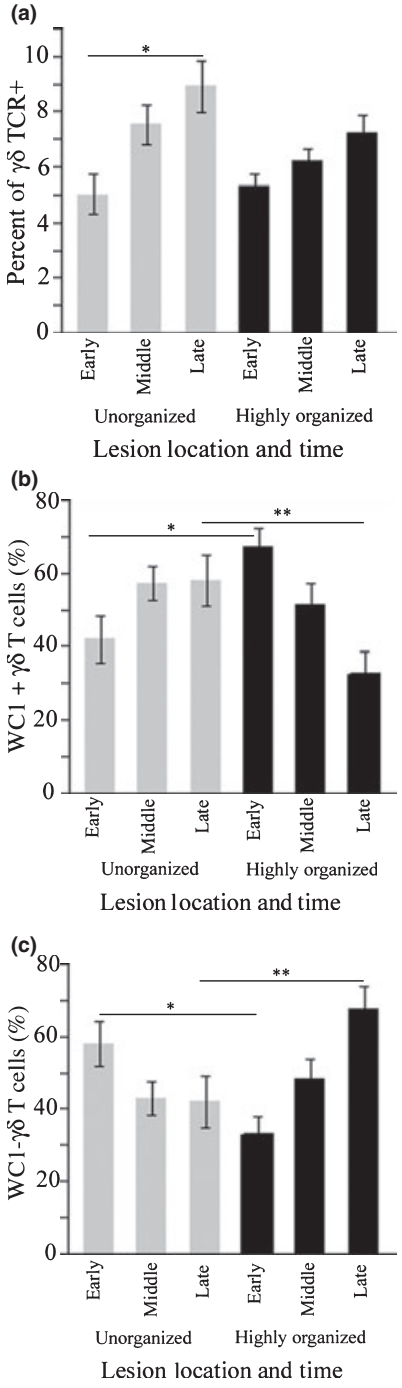

Figure 2 γδ T cell subsets in poorly organizing and highly organizing granulomas. In panel (a), the percentage of γδ T cells recruited to unorganized lesions was higher in late lesions compared with early lesions (*P = 0.0002). Panels (b) and (c) show that in comparison to unorganized sites, lesions that became highly organized were dominated initially by WC1 + γδ T cells (*P = 0.0062) and during later stages by WC1- γδ T cells (**P = 0.0017).

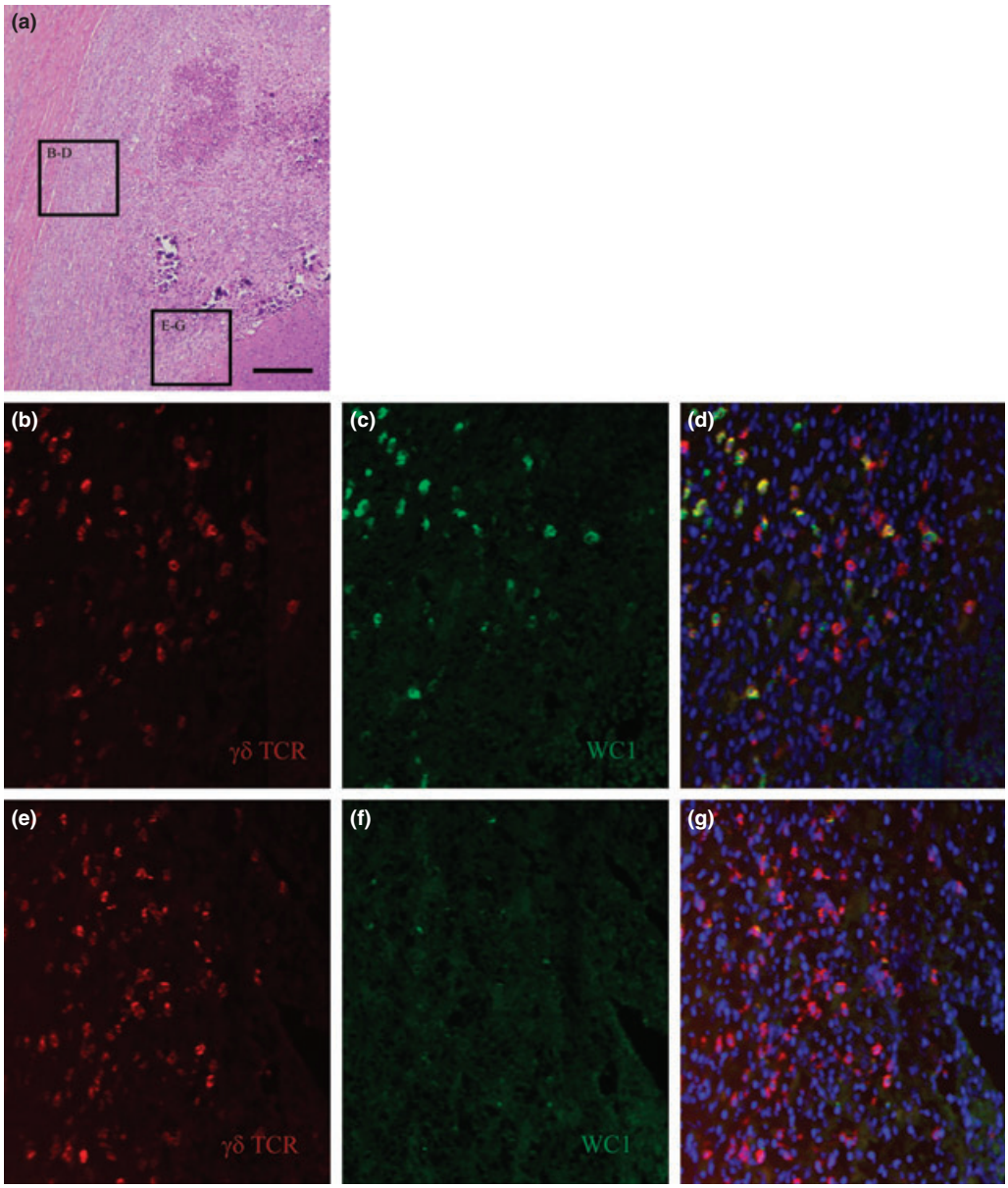

Figure 3 Spatial organization of γδ T cell subsets by immunofluorescent staining. Sections from highly organized granulomas examined for γδ T cell subset organization revealed distinct stratification patterns. Sections were taken from near the fibrous margin (panels b–d) or from near the necrotic centre (panels e–g) as indicated by the boxes in panel (a). The γδ TCR is labelled in red (panels b and e), WC1 is labelled in green (panels c and f) and nuclei are labelled blue in the overlay images (panels d and g). The WC1 + γδ T cells (red and green overlay) are limited to outer margins along the fibrous capsule while the lesion centres contain almost predominantly WC1- γδ T cells (single red staining). Bar = 200 μm.

stages of all lesions lacked significant histologic organization, and both γδ subsets were distributed evenly and diffusely throughout these sections. While the distribution of γδ T cell subsets remained diffuse over time in unorganized lesions, a distinct subset-specific stratification pattern was observed as granulomas exhibited progressive histologic organization. Specifically, the WC1 + subset was restricted to the outer margins of the granuloma near the fibrous border (Figure 3a–d) while WC1- cells were heavily concentrated near central regions of the granuloma adjacent to the area of central cavitation and necrosis (Figure 3a,e–g).

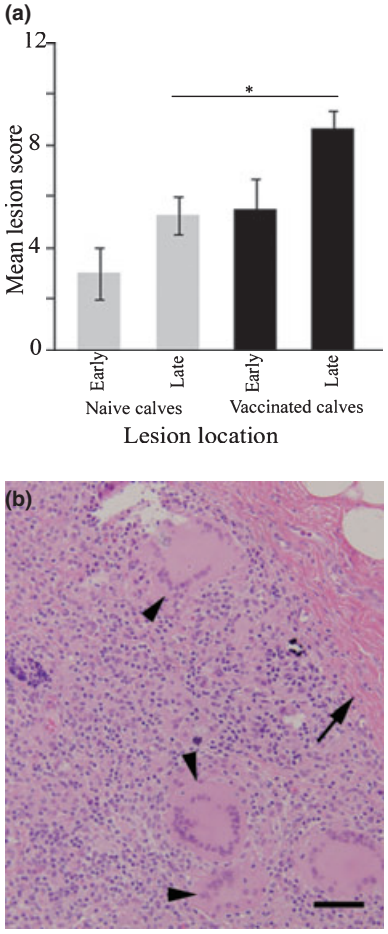

Figure 4 Histology of *Map* infection sites in naïve and vaccinated calves. Panel (a) shows lesion score summary; late stage lesions scored significantly higher in vaccinates compared with naïve calves (*P = 0.0449). Late stage *Map* infection site lesions in naïve calves were characterized by diffuse granulomatous inflammation (see Figure 1b) while *Map* infection sites in previously vaccinated calves (panel b) scored higher because of increased fibrous tissue (arrow) and prominent large multinucleated Langhans-type giant cells (arrow heads). Bar = 100 μm.

Histology of Map infection sites in naïve and vaccinated calves

We next set out to answer the question 'if calves initially produce a well-organized granuloma to *Map* vaccine, will they subsequently generate a highly organized granuloma to *Map* infection at a distant subcutaneous site?' We compared the histology of early and late *Map* infection sites in naïve calves to those in previously vaccinated calves. Regardless of the vaccination history of the animals, granulomas at *Map* infection sites did not achieve the same level of organization

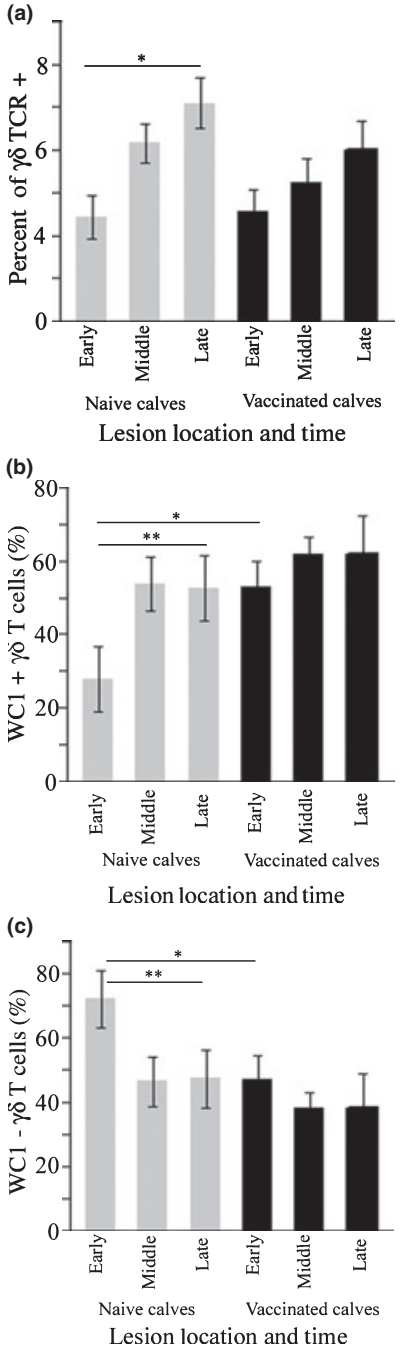

Figure 5 γδ T cell subsets in *Map* infection sites of naïve and vaccinated calves. The percentage of γδ T cells was significantly higher in late lesions compared to early lesions in naïve calves (panel a, *P = 0.0043) but not vaccinates. In panels b and c, WC1- γδ T cells were recruited more heavily to infection sites of naïve calves compared to vaccinates (*P < 0.05) and the number of WC1 + γδ T cells significantly increased over time in infection sites of naïve calves but not in vaccinates (**P < 0.05).

as the vaccine sites (Figure 1a). Nevertheless, we did find that at later time points, *Map* infection sites in vaccinated calves had significantly higher histologic scores compared to *Map* infection sites in naive calves (Figure 4a; $*P = 0.0449$). We examined the lesions to determine which parameter(s) of our scoring rubric (macrophages, lymphocytes, giant cells, fibrous tissue, necrosis and mineralization) accounted for differences observed. Late stage *Map* infection sites of vaccinated calves contained prominent large Langhans-type multinucleated giant cells (Figure 4b, arrowheads), mildly increased fibrosis (Figure 4b, arrow) and random small foci of necrosis. These parameters were not significant morphologic features of *Map* infection sites at any time point in naïve animals.

γδ T cell subsets in Map infection sites of naïve and vaccinated calves

Considering the effect of vaccination on *Map* granuloma morphology, we were interested to know if vaccination influenced recruitment of γδ T cell subsets to *Map* infection sites. We found the percentage of γδ T cells to be significantly greater in late stage lesions compared to early lesions in naïve calves (Figure 5a; $*P = 0.0043$) but not in vaccinates. When compared to vaccinated calves, the WC1- subset was more heavily recruited to early *Map* infection sites of naïve calves (Figure 5c; $*P < 0.05$), but the percentage of WC1- cells decreased over time. Though the WC1 + subset represented the minority of γδ T cells at early infection sites in naïve calves, the percentage of WC1 + cells increased significantly by the late stages of the infection sites (Figure 5b; $**P < 0.05$).

Discussion

Initial cellular interactions at mycobacterial infection sites are considered critical for generating effective and sustained protective immunity (Dieli *et al.* 2004), and an immunoregulatory role for γδ T lymphocytes in this process in humans and cattle has been proposed (Rhodes *et al.* 2001; Chen 2005; Born *et al.* 2006). Infection site immunopathology is difficult to investigate, and low numbers of γδ T cells in most species is an additional challenge to overcome for γδ T cell studies. As a result, γδ T cell studies have largely been limited to *in vitro* work using peripheral blood γδ T cells (mostly WC1 + in cattle and Vδ2 in humans) and have not examined γδ T cell subsets found in lower numbers in peripheral blood (bovine WC1- and human Vδ1). For example, bovine γδ T cells have been examined within mycobacterial granulomas, but these studies examined only WC1 + γδ T cells within granulomas of lymph nodes draining infection sites (Wangoo *et al.* 2005; Liebana *et al.* 2007; Palmer *et al.* 2007). We thus set out to use an *in vivo* system to build upon the knowledge gained from *in vitro* (peripheral blood) experiments. Our study is unique because it describes the *in vivo* recruitment of both WC1 + and WC1- γδ T cell subsets to mycobacterial infection sites in cattle with correlation to the morphology of developing granulomas. Using this model, we have previously described the histology of granulomas during generation and maintenance stages at subcutaneous infection sites by inducing granulomas on near-opposite ends of the morphologic spectrum. Specifically, *Map* vaccine induced well-organized granulomas resembling tuberculoid type while live *Map* induced unorganized granulomas resembling lepromatous type (Simutis *et al.* 2005; Lei *et al.* 2008). Further, we have shown a diminished phenotypic and functional maturation status of dendritic cell populations harvested from unorganized granulomas compared with those of well-organized granulomas (Lei *et al.* 2008). It has been shown that human γδ T cells are able to enhance dendritic cell maturation and thus effect initiation of the adaptive immune response (Ismaili *et al.* 2002; Munz *et al.* 2005; Devilder *et al.* 2006), though γδ T cell–dendritic cell interaction has not been fully investigated in the bovine.

In the present study, we have identified unique recruitment patterns of γδ T cell subsets that correlate to the degree of granuloma organization and provide evidence to suggest that previous antigen exposure influences recruitment of γδ T cells to an infection site. Lesions that progressed to highly organized granulomas in our study contained significantly more WC1 + γδ T cells at initial stages and significantly more WC1- γδ T cells during later stages. In contrast, lesions without progressive organization during the study demonstrated an inverse recruitment pattern of γδ T cells where WC1- cells predominated initially and WC1 + cells were found at elevated numbers at later stages. Progressive organization of the granuloma correlated to a distinct stratification pattern of γδ T cell subsets where WC1 + cells localized to marginal (peripheral) regions and WC1- cells accumulated adjacent to necrotic (central) regions. Finally, we observed that WC1- γδ T cells are transiently and preferentially recruited to early mycobacterial infection sites in naïve calves but not vaccinated calves. To our knowledge, this has not been previously described, but the observation is interesting as one feature of the tissue subset of human γδ T cells (Vδ1 cells compared to Vδ2 cells) is that they also seem to be preferentially recruited to local mycobacterial or viral infections (Modlin *et al.* 1989; Spada *et al.* 2000).

These findings suggest that subsets of γδ T cells play unique roles during the antimycobacterial immune response. Specifically, WC1- γδ T cells appear to have an enhanced ability to respond innately to live mycobacteria while WC1 + cells are best recruited after antigenic priming and we hypothesize that WC1 + cells function as early effector or memory cells during the immune response. A shift in the predominance of WC1 + to WC1- cells over time correlates to the transition from unorganized to a highly organized granuloma morphology. We believe this finding supports the hypothesis that γδ T cell subsets play a role in granuloma organization and/or maintenance during pathogenesis of mycobacterial disease, though further studies are needed for confirmation.

The ability to form organized granulomas to vaccine did not translate to an ability to generate highly organized granulomas to subsequent *Map* challenge. However, a significant difference in morphology of granulomas induced at *Map* infection sites in vaccinates but not naïve calves was the prominence of Langhans-type multinucleated giant cells. Giant cells are observed in a number of neoplastic or chronic inflammatory conditions of humans and animals, though few studies have examined inflammatory giant cells during mycobacterial infections (Zhu & Friedland 2006; Lay *et al.* 2007). A recent *in vitro* study reported that human macrophages responding to virulent mycobacteria (*M tuberculosis*) formed larger multinucleated cells with reduced phagocytic ability and elevated antigen presentation capacity compared to macrophages responding to avirulent mycobacteria (*M avium*). The authors noted that these giant cells resembled mature dendritic cells as a population of cells seemingly well-suited for enhanced antigen presentation and hypothesized an association with a stronger local host immune response (Lay *et al.* 2007). The presence of Langhans-type giant cells within *Map* vaccination sites and live *Map* infection sites of vaccinated but not naïve calves in our study is *in vivo* evidence to support the hypothesis that Langhans-type giant cells are indicative of the strength and possibly effectiveness of the local immune response, though to our knowledge this effect has not been definitively shown *in vivo* during the developing mycobacteria-induced lesions in a species other than bovine.

We recognize that anatomic and immunologic variables existing between our model (skin) and the natural infection site (intestine) may alter the host immune response at these locations. In addition, we know that vaccine adjuvant further influences the local immune response, and thus we do not attribute the final consequences of the infection site granuloma in our model to any one component of the host immune response described in this work. However, we believe, this study demonstrates important features of γδ T cell recruitment within unorganized and highly organized granulomas at sites of mycobacterial-induced inflammation. We are now working towards understanding the functions of these γδ subsets and how they influence the induction of either protective or non-protective immune responses to mycobacterial diseases.

References

Battistini L., Caccamo N., Borsellino G. *et al.* (2005) Homing and memory patterns of human gammadelta T cells in physiopathological situations. *Microbes. Infect.* **7**, 510–517.

Blumerman S.L., Herzig C.T., Rogers A.N., Telfer J.C., Baldwin C.L. (2006) Differential TCR gene usage between WC1- and WC1 + ruminant gammadelta T cell subpopulations including those responding to bacterial antigen. *Immunogenetics* **58**, 680–692.

Born W.K., Reardon C.L., O'Brien R.L. (2006) The function of gammadelta T cells in innate immunity. *Curr. Opin. Immunol.* **18**, 31–38.

Brandes M., Willimann K., Moser B. (2005) Professional antigen-presentation function by human gammadelta T Cells. *Science* **309**, 264–268.

Chen Z.W. (2005) Immune regulation of gammadelta T cell responses in mycobacterial infections. *Clin. Immunol.* **116**, 202–207.

Chen Z.W. & Letvin N.L. (2003) Adaptive immune response of Vgamma2Vdelta2 T cells: a new paradigm. *Trends Immunol.* **24**, 213–219.

Co D.O., Hogan L.H., Kim S.I., Sandor M. (2004) Mycobacterial granulomas: keys to a long-lasting host-pathogen relationship. *Clin. Immunol.* **113**, 130–136.

Das H., Sugita M., Brenner M.B. (2004) Mechanisms of Vdelta1 gammadelta T cell activation by microbial components. *J. Immunol.* **172**, 6578–6586.

Devilder M.C., Maillet S., Bouyge-Moreau I., Donnadieu E., Bonneville M., Scotet E. (2006) Potentiation of antigen-stimulated V gamma 9V delta 2 T cell cytokine production by immature dendritic cells (DC) and reciprocal effect on DC maturation. *J. Immunol.* **176**, 1386–1393.

Dieli F., Poccia F., Lipp M. *et al.* (2003) Differentiation of effector/memory Vdelta2 T cells and migratory routes in lymph nodes or inflammatory sites. *J. Exp. Med.* **198**, 391–397.

Dieli F., Caccamo N., Meraviglia S. *et al.* (2004) Reciprocal stimulation of gammadelta T cells and dendritic cells during the anti-mycobacterial immune response. *Eur. J. Immunol.* **34**, 3227–3235.

Emile J.F., Patey N., Altare F. *et al.* (1997) Correlation of granuloma structure with clinical outcome defines two types of idiopathic disseminated BCG infection. *J. Pathol.* **181**, 25–30.

Endsley J.J., Waters W.R., Palmer M.V. *et al.* (2009) The calf model of immunity for development of a vaccine against tuberculosis. *Vet. Immunol. Immunopathol.* **128**, 199–204.

Hedges J.F., Cockrell D., Jackiw L., Meissner N., Jutila M.A. (2003) Differential mRNA expression in circulating gammadelta T lymphocyte subsets defines unique tissue-specific functions. *J. Leukoc. Biol.* **73**, 306–314.

Hedges J.F., Lubick K.J., Jutila M.A. (2005) Gamma delta T cells respond directly to pathogen-associated molecular patterns. *J. Immunol.* **174**, 6045–6053.

Hoft D.F., Brown R.M., Roodman S.T. (1998) Bacille Calmette–Guerin vaccination enhances human gamma delta T cell responsiveness to mycobacteria suggestive of a memory-like phenotype. *J. Immunol.* **161**, 1045–1054.

Ismaili J., Olislagers V., Poupot R., Fournie J.J., Goldman M. (2002) Human gamma delta T cells induce dendritic cell maturation. *Clin. Immunol.* **103**, 296–302.

Johnson L., Gough J., Spencer Y., Hewinson G., Vordermeier M., Wangoo A. (2006) Immunohistochemical markers augment evaluation of vaccine efficacy and disease severity in bacillus Calmette–Guerin (BCG) vaccinated cattle challenged with *Mycobacterium bovis*. *Vet. Immunol. Immunopathol.* **111**, 219–229.

Johnson W.C., Bastos R.G., Davis W.C., Goff W.L. (2008) Bovine WC1(-) gammadelta T cells incubated with IL-15 express the natural cytotoxicity receptor CD335 (NKp46) and produce IFN-gamma in response to exogenous IL-12 and IL-18. *Dev. Comp. Immunol.* **32**, 1002–1010.

Kennedy H.E., Welsh M.D., Bryson D.G. *et al.* (2002) Modulation of immune responses to *Mycobacterium bovis* in cattle depleted of WC1(+) gamma delta T cells. *Infect. Immun.* **70**, 1488–1500.

Lammas D.A., De Heer E., Edgar J.D. *et al.* (2002) Heterogeneity in the granulomatous response to mycobacterial infection in patients with defined genetic mutations in the interleukin 12-dependent interferon-gamma production pathway. *Int. J. Exp. Pathol.* **83**, 1–20.

Lay G., Poquet Y., Salek-Peyron P. *et al.* (2007) Langhans giant cells from M. tuberculosis-induced human granulomas cannot mediate mycobacterial uptake. *J. Pathol.* **211**, 76–85.

Lei L., Plattner B.L., Hostetter J.M. (2008) Live *Mycobacterium avium* subsp. paratuberculosis and a killed-bacterium vaccine induce distinct subcutaneous granulomas, with unique cellular and cytokine profiles. *Clin. Vaccine Immunol.* **15**, 783–793.

Liebana E., Aranaz A., Aldwell F.E. *et al.* (2000) Cellular interactions in bovine tuberculosis: release of active mycobacteria from infected macrophages by antigen-stimulated T cells. *Immunology* **99**, 23–29.

Liebana E., Marsh S., Gough J. *et al.* (2007) Distribution and Activation of T-lymphocyte Subsets in tuberculous bovine lymph-node granulomas. *Vet. Pathol.* **44**, 366–372.

Machugh N.D., Mburu J.K., Carol M.J., Wyatt C.R., Orden J.A., Davis W.C. (1997) Identification of two distinct subsets of bovine gamma delta T cells with unique cell surface phenotype and tissue distribution. *Immunology* **92**, 340–345.

Meissner N., Radke J., Hedges J.F. *et al.* (2003) Serial analysis of gene expression in circulating gamma delta T cell subsets defines distinct immunoregulatory phenotypes and unexpected gene expression profiles. *J. Immunol.* **170**, 356–364.

Modlin R.L., Pirmez C., Hofman F.M. *et al.* (1989) Lymphocytes bearing antigen-specific gamma delta T-cell receptors accumulate in human infectious disease lesions. *Nature* **339**, 544–548.

Morita C.T., Beckman E.M., Bukowski J.F. *et al.* (1995) Direct presentation of nonpeptide prenyl pyrophosphate antigens to human gamma delta T cells. *Immunity* **3**, 495–507.

Munz C., Steinman R.M., Fujii S. (2005) Dendritic cell maturation by innate lymphocytes: coordinated stimulation of innate and adaptive immunity. *J. Exp. Med.* **202**, 203–207.

Palmer M.V., Waters W.R., Thacker T.C. (2007) Lesion development and immunohistochemical changes in granulomas from cattle experimentally infected with *Mycobacterium bovis*. *Vet. Pathol.* **44**, 863–874.

Price S.J., Hope J.C. (2008) Enhanced secretion of interferon-gamma by bovine gammadelta T cells induced by coculture with *Mycobacterium bovis*-infected dendritic cells: evidence for reciprocal activating signals. *Immunology* **126**, 201–208.

Price S.J., Sopp P., Howard C.J., Hope J.C. (2007) Workshop cluster 1 + gammadelta T-cell receptor T cells from calves express high levels of interferon-gamma in response to stimulation with interleukin-12 and -18. *Immunology* **120**, 57–65.

Puan K.J., Jin C., Wang H. *et al.* (2007) Preferential recognition of a microbial metabolite by human V{gamma}2V{delta}2 T cells. *Int. Immunol.* **19**, 657–673.

Rhodes S.G., Hewinson R.G., Vordermeier H.M. (2001) Antigen recognition and immunomodulation by gamma delta T cells in bovine tuberculosis. *J. Immunol.* **166**, 5604–5610.

Rogers A.N., VanBuren D.G., Hedblom E., Tilahun M.E., Telfer J.C., Baldwin C.L. (2005a) Function of ruminant gammadelta T cells is defined by WC1.1 or WC1.2 isoform expression. *Vet. Immunol. Immunopathol.* **108**, 211–217.

Rogers A.N., Vanburen D.G., Hedblom E.E., Tilahun M.E., Telfer J.C., Baldwin C.L. (2005b) Gammadelta T cell function varies with the expressed WC1 coreceptor. *J. Immunol.* **174**, 3386–3393.

Russell D.G. (2007) Who puts the tubercle in tuberculosis? *Nat. Rev. Microbiol.* **5**, 39–47.

Saunders B.M., Britton W.J. (2007) Life and death in the granuloma: immunopathology of tuberculosis. *Immunol. Cell Biol.* **85**, 103–111.

Shen Y., Zhou D., Qiu L. *et al.* (2002) Adaptive immune response of Vgamma2Vdelta2 + T cells during mycobacterial infections. *Science* **295**, 2255–2258.

Simutis F.J., Cheville N.F., Jones D.E. (2005) Investigation of antigen-specific T-cell responses and subcutaneous granuloma development during experimental sensitization of calves with *Mycobacterium avium* subsp paratuberculosis. *Am. J. Vet. Res.* **66**, 474–482.

Smyth A.J., Welsh M.D., Girvin R.M., Pollock J.M. (2001) In vitro responsiveness of gammadelta T cells from *Mycobacterium bovis*-infected cattle to mycobacterial antigens: predominant involvement of WC1(+) cells. *Infect. Immun.* **69**, 89–96.

Spada F.M., Grant E.P., Peters P.J. *et al.* (2000) Self-recognition of CD1 by gamma/delta T cells: implications for innate immunity. *J. Exp. Med.* **191**, 937–948.

Tanaka S., Itohara S., Sato M., Taniguchi T., Yokomizo Y. (2000) Reduced formation of granulomata in gamma(delta) T cell knockout BALB/c mice inoculated with *Mycobacterium avium* subsp. paratuberculosis. *Vet. Pathol.* **37**, 415–421.

Wangoo A., Johnson L., Gough J. *et al.* (2005) Advanced granulomatous lesions in *Mycobacterium bovis*-infected cattle are associated with increased expression of type I procollagen, gammadelta (WC1 +) T cells and CD 68 + cells. *J. Comp. Pathol.* **133**, 223–234.

Welsh M.D., Kennedy H.E., Smyth A.J., Girvin R.M., Andersen P., Pollock J.M. (2002) Responses of bovine WC1(+) gammadelta T cells to protein and nonprotein antigens of *Mycobacterium bovis*. *Infect. Immun.* **70**, 6114–6120.

Wijngaard P.L., MacHugh N.D., Metzelaar M.J. *et al.* (1994) Members of the novel WC1 gene family are differentially expressed on subsets of bovine CD4-CD8-gamma delta T lymphocytes. *J. Immunol.* **152**, 3476–3482.

Wilson E., Aydintug M.K., Jutila M.A. (1999) A circulating bovine gamma delta T cell subset, which is found in large numbers in the spleen, accumulates inefficiently in an artificial site of inflammation: correlation with lack of expression of E-selectin ligands and L-selectin. *J. Immunol.* **162**, 4914–4919.

Zhu X.W., Friedland J.S. (2006) Multinucleate giant cells and the control of chemokine secretion in response to *Mycobacterium tuberculosis*. *Clin. Immunol.* **120**, 10–20.

